
Measurement of the Shapiro Time Delay Between Drag-Free Spacecraft

Neil Ashby¹ and Peter L. Bender²

¹ Department of Physics, UCB 390, University of Colorado, Boulder, CO 80309-0390, USA

² JILA, UCB 440, University of Colorado, Boulder, CO 80309-0440, USA

Summary. In 1964 Shapiro pointed out that γ can be determined from measurements of the relativistic time delay for electromagnetic waves passing near a massive body such as the Sun. The delay for two-way measurements from Earth to a spacecraft passing behind the Sun can be more than 200 μs . Microwave range and range-rate measurements of this kind from Earth to several spacecraft have provided our best information so far on γ . Laser time-delay measurements and determinations of the deflection of laser beams near the Sun also have been proposed. A mission of this kind called Laser Astrometric Test of Relativity (LATOR) currently is being considered. Here we discuss a considerably different mission which would use drag-free spacecraft, whose orbits can be accurately determined, to measure the Shapiro time delay for laser beams passing near the Sun. One spacecraft would be located near the L1 Lagrange point, between the Earth and the Sun. The other would be launched into an orbit similar to the ones used in LATOR, with 1.5 year period and eccentricity such that three occultations by the Sun would occur within 2 years after launch. We also consider higher-order time-delay effects. In the present experiment laser signals are sent from a drag-free spacecraft at the L1 point, and transponded back by a drag-free spacecraft passing behind the Sun. A high-stability frequency standard located on the L1 spacecraft permits accurate measurement of the time delay. Both spacecraft are designed for extremely low spurious accelerations at periods out to roughly 20 days.

1 Introduction

Historically, the first accurate measurements of the Shapiro time delay [1] were made using microwave range measurements to the Mariner 9 spacecraft orbiting around Mars [2, 3] and to the Viking Orbiters and Landers [3–5]. Recently, a measurement of the spatial curvature parameter γ with $2.3 \cdot 10^{-5}$ accuracy was made during the Cassini mission [6]. The time derivative of the time delay was measured from Doppler shifts in microwave signals sent from Earth to a transponder on the spacecraft and back. Great care was taken to minimize spurious effects due to the Earth's atmosphere and to the

interplanetary electron density. An additional improvement in the accuracy for γ to roughly $1 \cdot 10^{-6}$ is expected from measurement of the gravitational deflection of light rays during the GAIA astrometric mission of the European Space Agency.

The LATOR experiment [7–9] is intended to give further improvements in the measurement of γ . It involves placing two spacecraft in very similar solar orbits with periods of 1.5 years. The orbits can be chosen so that the spacecraft make three passes behind the Sun during a 7-month period centered on 18 months after launch, and the angular separation between them as seen from Earth is roughly 1° . An optical interferometer on the International Space Station observes laser beams from the two distant spacecraft and would measure the angular separation between the spacecraft with high accuracy. The lengths of the three sides of the triangle would be measured with lasers. From the non-Euclidian geometry of the triangle when one arm passes near the Sun, γ can be determined.

As an alternate approach, we consider making Shapiro time-delay measurements from a satellite near the L1 point of the Earth–Sun system to a single transponder spacecraft in a LATOR-type orbit when the line of sight passes near the Sun. The L1 spacecraft would have a high-stability atomic frequency standard with performance similar to that expected for the cooled Cs clocks that have been developed for the ACES [10] and the PARCS experiments [11] on the International Space Station. Both the distant spacecraft and the L1 spacecraft would be designed to have very low levels of nongravitational orbit disturbances. The atomic frequency standard would need to be quite small, but the environmental disturbances near the L1 point would be considerably lower than those on the Space Station.

The size of the Shapiro time delay and its variation with time for the LATOR-type orbit of the distant spacecraft will be discussed in Sect. 2. In Sect. 3, the expected signal-to-noise ratio will be derived for determining γ from an idealized Gravitational Time Delay (GTD) mission. For this ideal case, only white frequency noise in the clock on the L1 spacecraft is allowed for. In Sect. 4, the requirements on the drag-free systems to minimize nongravitational accelerations of the spacecraft will be considered, along with possible excess clock noise at very low frequencies. Then, the limitations from the actual time-delay measurement method will be discussed in Sect. 5. The overall results will be summarized in Sect. 6.

2 Shapiro Time Delay

Because of the sensitivity of the measurements discussed in this chapter, we have performed a more accurate calculation of the Shapiro time delay than is quoted in many textbooks. Usually a “straight line” approximation is used, in which the delay is calculated assuming the path of the photon is straight [1]. A more careful calculation including the bending of the path shows that

there is an additional contribution of first order in the quantity GM_\odot/c^3 . For example, Weinberg gives the following expression for the time delay required for a photon to pass from the point of closest approach to the Sun, at $r = b$, to the radius r [12]:

$$\Delta t_{\text{delay}}^{(1)} = (1 + \gamma) \frac{GM_\odot}{c^3} \ln \left(\frac{r + \sqrt{r^2 - b^2}}{b} \right) + (1 + \gamma) \frac{GM_\odot}{c^3} \sqrt{\frac{r - b}{r + b}}. \quad (1)$$

The last term in this result can amount to tens of microseconds. The result is expressed in the isotropic coordinates that are customarily used when discussing time-delay observations.

Because of its possible importance in solar system time-delay observations, we have extended the delay calculation to higher order. We briefly describe the method here. If the Sun is taken to be a spherically symmetric mass source, then the motion of a photon can be assumed to lie in the $\theta = \pi/2$, equatorial plane. Also, in isotropic coordinates the metric does not depend explicitly on coordinate time or on azimuthal angle. The cyclic nature of these two coordinates leads immediately to two constants of the motion, corresponding roughly to energy and angular momentum. These two constants allow the azimuthal angle and the scalar orbit parameter to be eliminated in favor of the coordinate time. Since the path followed by a photon is a null geodesic, there results a first-order differential equation for dt/dr , where t is the coordinate time ($x^0 = ct$). Contributions to this equation can be expanded in powers of $\mu = GM_\odot/c^2$ and the equation can be integrated. The result of these calculations gives for the next-order contribution to time delay [13]

$$\begin{aligned} \Delta t_{\text{delay}}^{(2)} = & \frac{(3\delta/2 + 4(\gamma + 1) - 2\beta)(GM_\odot)^2}{bc^5} \text{ArcTan} \left(\frac{\sqrt{r^2 - b^2}}{b} \right) \\ & - \frac{(\gamma + 1)^2(GM_\odot)^2}{2bc^5} \left(2 + \frac{b}{r + b} \right), \end{aligned} \quad (2)$$

where β is a PPN parameter measuring the strength of the nonlinear term in g_{00} , and δ is defined by expanding the isotropic metric component g_{11} to higher order:

$$g_{11}(r) = 1 + \frac{2\gamma\mu}{r} + \frac{3\delta\mu^2}{r^2}. \quad (3)$$

In general relativity, $\delta = 1$.

Figure 1 shows the second-order time-delay contributions of (2) for several different values of the distance of closest approach, b . The three curves, upper to lower, correspond, respectively, to $b = 1.1, 1.2, 1.3$ solar radii, and the quantity plotted is (2) in picoseconds, for the delay during one-way travel from the point of closest approach to the radial distance r . The horizontal axis is the final radial distance expressed in units of the solar radius. In the experiment proposed here, this delay will contribute four times, so the total second-order

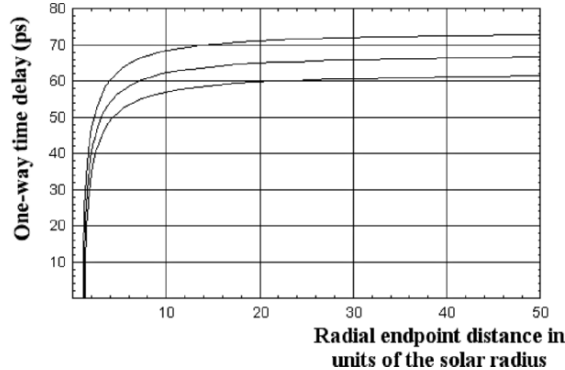


Fig. 1. Second-order contributions to time delay for one-way passage of a photon from the point of closest approach to a radial distance r from the Sun.

delay can amount to about a quarter of a microsecond, and certainly has to be taken into account. The effect of a deviation $\gamma - 1$ on these contributions is negligible.

We have also estimated the time delay due to the solar quadrupole moment. Such contributions are controlled by the parameter

$$\frac{GM_{\odot} J_2 a_1^2}{b^2 c^3} < 10^{-12} \text{ s}, \quad (4)$$

where $J_2 \approx 2 \cdot 10^{-7}$ is the Sun's quadrupole moment coefficient and a_1 is the Sun's equatorial radius. There is a complicated dependence of this delay on the orientation of the Sun's rotation axis with respect to the photon's path, but the net effect is only 2 or 3 ps and we shall not consider it further.

In the present modification of the LATOR mission, the line of sight from the spacecraft at L1 to the distant spacecraft passes across the Sun three times. Figure 2 plots the total Shapiro time delay in microseconds, and the angle (in milliradians) between the line to the Sun's center and the line to the occulted spacecraft. Both first-order contributions of (1) are included. The second-order effects are too small to see on the graph.

This figure shows that during conjunctions the time delay is, to a very good approximation, symmetric about the time t_0 when the distant spacecraft is exactly behind the center of the Sun. The logarithm clearly dominates the time dependence. For purposes of analysis in the following sections, we have found that the time-delay function, within a span of ± 20 days on either side of t_0 , can be fit very well by a function of the form

$$0.97 \cdot \frac{8GM}{c^3} \ln(R|t - t_0|) + \text{const.}, \quad (5)$$

where R is the rate of motion of the line of sight with respect to the Sun's center in solar radii per day, and t is in days. The constant is not important

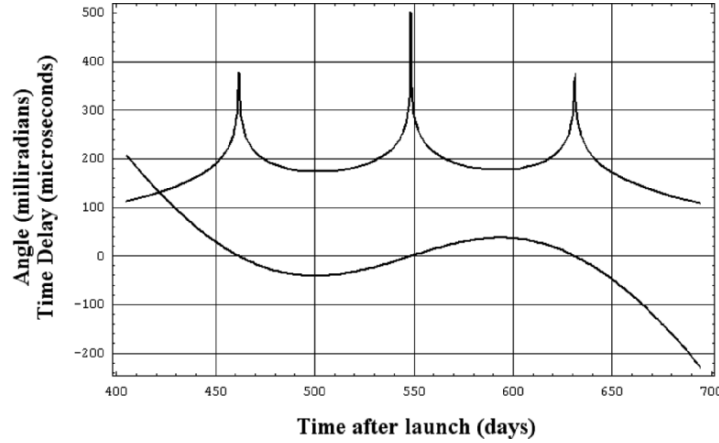


Fig. 2. Plots of the first-order time delay (in microseconds) as the occulted spacecraft passes behind the Sun, and the angle between the line from L1 to the Sun and the line from L1 to the distant spacecraft (in milliradians).

when discussing uncertainties, since it would represent a constant bias in the time delay. The logarithmic dependence is the distinctive time signature for the Shapiro effect, and we shall henceforth drop the constant.

3 Idealized Gravitational Time-Delay Mission

Most of the accuracy for determining the relativistic time delay is expected to come from a period of roughly 20 days around the time of passage of the line of sight behind the Sun, as will be discussed later. Thus the noise in the frequency standard and in displacements of the spacecraft due to nongravitational accelerations will be of interest at frequencies down to about $5 \cdot 10^{-7}$ Hz. It is assumed that the measurements will be made continuously from time $-t_2$ to $-t_1$ and from time t_1 to t_2 , where $t = 0$ when the line of sight between the spacecraft passes through the center of the Sun.

For simplicity, the distance between the spacecraft is assumed to be constant except for the relativistic time delay. The time signature of $\gamma^* = (\gamma+1)/2$ is taken to be

$$g(t) = -B(\ln |Rt| - M), \quad (6)$$

where $M = \langle \ln |Rt| \rangle$ is the mean value of $\ln |Rt|$ over the periods $-t_2$ to $-t_1$ and t_1 to t_2 , and $B = 0.97 \cdot 8GM_{\odot}/c^3 = 3.82 \cdot 10^{-5}$ s.

The rate at which the line of sight to the distant spacecraft passes across the Sun varies substantially between the three conjunctions with the Sun, with the second one having a considerably lower rate than the other two. In solar radii per day, the rate for the first and third conjunctions is about 0.7, and we will assume this value for our reference case. To avoid measurements

closer than 0.4 solar radii from the limb, we chose to make t_1 be 2 days after t_0 and t_2 be 10 days after t_0 . For the second conjunction, the rate would be only about 0.2 solar radii per day.

In the reference case, we assume that the only noise in the measurements is white fractional frequency noise $n(f)$ at a level of $1 \cdot 10^{-13} \text{ Hz}^{-1/2}$ at all frequencies. This is close to the noise level expected for the ACES and PARCS clocks [10,11] at frequencies above $5 \cdot 10^{-7} \text{ Hz}$. This noise affects the results in two ways. One is the jitter in the measured round-trip travel time of roughly 2,000–2,200 s due to the phase jitter in the output from the frequency standard. However, this error is reduced strongly when the measurements are averaged over periods of hours. The other, more serious, noise is the variations in the frequency over the whole measurement time. If the frequency of the standard is different near the end of the measurement time from what it was earlier in the measurement period, the measured total travel time will be affected proportionately.

The usual method of optimal filtering (see, e.g., [14] and references therein) would be used to determine the value of γ^* . Let $g(f)$ be the Fourier transform of $g(t)$ over the time of the measurements. Then the square of the signal-to-noise ratio is given by

$$\left(\frac{S}{N}\right)^2 = \int_0^\infty \frac{2|g(f)|^2}{n(f)^2} df. \quad (7)$$

We also assume for the reference case that $t_1 = 2$ days and $t_2 = 10$ days. Because of the symmetry of the signal before and after $t = 0$, only the cosine terms of $g(f)$ are nonzero

$$g(f) = 2 \int_{t_1}^{t_2} g(t) \cos(\omega t) dt, \quad (8)$$

where $\omega = 2\pi f$. The factor 2 comes from time symmetry of the time-delay signal.

Since $n(f)$ is assumed to be independent of frequency in the reference case, it can be taken outside the integral in (7):

$$\left(\frac{S}{N}\right)^2 = \frac{2}{n(f)^2} \int_0^\infty g(f)^2 df, \quad (9)$$

and Parseval's theorem implies:

$$\int_0^\infty g(f)^2 df \approx 2\pi \int_{t_1}^{t_2} g(t)^2 dt. \quad (10)$$

After some algebra,

$$\begin{aligned} \int_{t_1}^{t_2} g(t)^2 dt = & B^2 R(t_2(\ln(Rt_2)))^2 - t_1(\ln(Rt_1))^2 - 2(t_2 \ln(Rt_2) - t_1 \ln(Rt_1)) \\ & + 2(t_2 - t_1) - M^2(t_2 - t_1) \end{aligned} \quad (11)$$

where M is the mean value

$$M = (t_2 \ln(Rt_2) - t_1 \ln(Rt_1)) / (t_2 - t_1) - 1. \quad (12)$$

From the above,

$$\int_{t_1}^{t_2} g(t)^2 dt = B^2 R \left((t_2 - t_1) - (t_2 t_1 / (t_2 - t_1)) (\ln(Rt_2) - \ln(Rt_1))^2 \right). \quad (13)$$

For our reference case, $t_2 = 8.64 \cdot 10^5$ s, $t_1 = 1.728 \cdot 10^5$ s, and

$$\int_0^\infty g(f)^2 df = 2\pi \cdot 1.317 \cdot 10^5 B^2 (s^3). \quad (14)$$

Because only the cosine terms in the noise contribute, the effective noise level is reduced from $1 \cdot 10^{-13}$ to $0.71 \cdot 10^{-13}$ Hz $^{-1/2}$. Since the total round-trip time is about 2,200 s for the first and third conjunctions, the noise in measuring it is

$$n(f) = 1.56 \cdot 10^{-10} \text{ s Hz}^{-1/2}. \quad (15)$$

Thus, from (9), (10), and (13),

$$(S/N)^2 = 1.655 \cdot 10^6 B^2 / [2.42 \cdot 10^{-20}] = 9.3 \cdot 10^{16}. \quad (16)$$

This corresponds to an idealized precision of $0.33 \cdot 10^{-8}$ for determining γ^* , or $0.66 \cdot 10^{-8}$ for γ .

4 Effects of Nongravitational Accelerations

For the GTD mission, the level of nongravitational accelerations of the spacecraft has to be kept very low out to long periods. For comparison, a joint mission of the European Space Agency and NASA called the Laser Interferometer Space Antenna (LISA) [15] has a requirement of less than $3 \cdot 10^{-15}$ m s $^{-2}$ Hz $^{-1/2}$ for the spurious accelerations of proof masses aboard each spacecraft at frequencies down to 0.1 mHz [16]. Each spacecraft is servocontrolled to follow the average position of two proof masses inside it to roughly $3 \cdot 10^{-9}$ m Hz $^{-1/2}$. This is done by a disturbance reduction system (DRS) (“drag-free” system) [17] that uses micronewton thrusters to cancel out the solar radiation pressure force and other nongravitational forces on the spacecraft. The relative displacements of the spacecraft with respect to the proof masses are determined by two gravitational reference sensors (GRSs) [18, 19] containing the proof masses. For the GTD mission, only a single GRS would be needed on each spacecraft.

Below 0.1 mHz, it has been suggested [20] that a spurious acceleration level increasing only as $((0.1 \text{ mHz})/f)^{0.5}$ between 0.1 and 0.003 mHz could be achieved with only moderate additional experimental constraints. At still

lower frequencies, we assume that the acceleration level will increase as $(0.003 \text{ mHz})/f$. If $a(f)$ is the spurious acceleration level at frequency f for the GRS on each spacecraft, the resulting noise level in the round-trip distance between the spacecraft will be

$$x(f) = 2\sqrt{2} \frac{a(f)}{\omega^2}. \quad (17)$$

The equivalent time-delay noise $p(f) = x(f)/c$ will cross the value of $n(f) = 1 \cdot 10^{-13} \text{ Hz}^{-1/2}$ that we have adopted at a frequency of $4.0 \cdot 10^{-7} \text{ Hz}$, and near that frequency it is given by

$$p(f) = 2 \cdot 10^{-10} (4.0 \cdot 10^{-7} \text{ Hz}/f)^3 \text{ s Hz}^{-1/2}. \quad (18)$$

In view of the rapid increase of $p(f)$ with decreasing f , we can approximate its effect by cutting off the integral in (2) on the lower end at $4.0 \cdot 10^{-7} \text{ Hz}$. To see what the effect of the assumed level of spurious accelerations is, we have calculated $g(f)$ from (3) and then numerically integrated the function $(g(f)/B)^2$. The dependence of this function on f is shown in Fig. 3. The total integral is $8.1 \cdot 10^5 \text{ s}$, in good agreement with (14), and the fraction of the integral from frequencies below $4 \cdot 10^{-7} \text{ Hz}$ is only about 5%. Thus the effect of limitations from the spurious accelerations of the spacecraft appears to be small, if the assumed performance level for the DRSs can be achieved. At the very low acceleration levels and frequencies involved, verification of the necessary performance will have to be achieved from modeling rather than direct testing, but this approach seems quite feasible for the types of forces involved.

The most serious challenge for the DRS at the lowest frequencies is likely to be the rate of change of the solar intensity at the distant spacecraft. During the 20 day periods around the first and third solar conjunctions, the equilibrium temperature of the spacecraft would change by roughly 8 K if special measures were not taken. To minimize the effect on the GRS, both active temperature

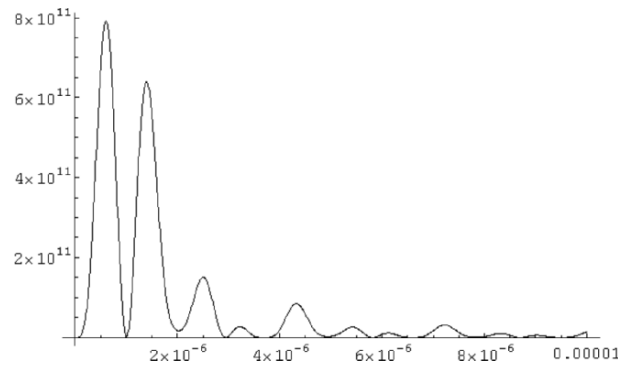


Fig. 3. Plot of the function $g(f)^2/B^2$ for frequencies up to 0.01 mHz.

control of the spacecraft and careful design to minimize temperature gradients across the GRS will be needed.

5 Other Time-Delay Measurement Errors

One method for measuring the time delay for signals sent between spacecraft that are far apart is the use of pulsed lasers. Lasers giving 100 ps pulses in the green with 0.1 J per pulse energy and 20 Hz repetition rate are available commercially. We assume that a laser giving a train of such pulses is located on each spacecraft, and that a fast detector measures the time delay between the receipt of a pulse and the next pulse generated onboard. The expected accuracy is 5 ps or better. For the round-trip travel time, the resulting contribution of the timing to the error will be 10 ps or less.

It is difficult to know what should be assumed concerning the time variation of pulse timing errors, since they may well be systematic in nature. During the time of perhaps 8 days for the line of sight between the two spacecraft to go from 0.4 to 6.0 times the solar radius from the limb, the change in the round-trip time delay will be about $6.4 \cdot 10^{-5}$ s. Thus a drift of 10 ps in the timing error over this time, and an opposite sign drift during the corresponding time before conjunction, could give as much as a roughly $3 \cdot 10^{-7}$ error in γ . This is what would result from treating the timing error as a worst case error, in terms of its time dependence. An error this large is unlikely, and some additional reduction in the timing system error probably is possible by improvements in the system design. However, to achieve an accuracy of better than $1 \cdot 10^{-7}$ for γ for the reference case would require a substantial improvement in the travel time measurement approach.

In view of this situation, it is also desirable to investigate what could be done with a cw laser travel time measurement system. The system we will consider consists of taking perhaps 0.5 W of cw output at 1,030 or 1,064 nm wavelength from a frequency-stabilized YbYAG or NdYAG laser on each spacecraft and putting it through an electrooptic phase modulator. Such modulators at frequencies up to 40 GHz are now commercially available, and probably will be space qualified in the next few years. This is because of strong interest in laser communications at high data rates between spacecraft. A short Fabry–Perot interferometer would be included after the modulator to pass the two sidebands and strongly suppress the carrier. The beam would then be sent to the distant spacecraft through a roughly 100 mm diameter transmitting telescope. A separate 100 mm diameter receiving telescope, with careful attention to reducing the effect of scattered sunlight hitting the entrance aperture, also would be provided on each spacecraft, to minimize the problem of making measurements near the limb of the Sun.

To detect changes in the round-trip travel time, it would be necessary to compensate for the Doppler shifts in the received signals. The one-way Doppler shifts near the times of the first and third solar conjunctions will be up to

about 5 GHz. This can be compensated for by adding additional sidebands to the local oscillator laser beams. With corrections, the phase difference of the two beat notes measured at each end of the path would give a measure of the time delay over the path. For a modulation frequency of 40 GHz and sidebands 80 GHz apart, the sum of the phase differences would change by 1 cycle each time the round-trip time changes by 12.5 ps. Measurement of the phase differences to 5° accuracy on each spacecraft would correspond to less than a 0.35 ps measurement error for the round-trip time delay. If a drift in the error of this magnitude occurred over the 8 days of the measurements before conjunction and an opposite drift occurred during the measurements after conjunction, this would give a worst case error of $1.1 \cdot 10^{-8}$ for γ . However, a one-sigma error estimate of $0.4 \cdot 10^{-8}$ for γ from this error source seems reasonable.

Another benefit of an improved travel time measurement method is related to the stability requirements for the L1 clock. We assumed earlier that a power spectral amplitude of $1 \cdot 10^{-13} \text{ Hz}^{-1/2}$ for the performance of the L1 clock can be maintained at frequencies down to about $4 \cdot 10^{-7} \text{ Hz}$. Laboratory data on this seem quite encouraging, but as for spurious acceleration sources, considerable reliance on modeling of the disturbing effects at low frequencies may be needed. On the other hand, checks on the clock stability on orbit may be possible by sending optical timing signals from the Earth to the L1 spacecraft and back. If measurements of roughly 2 ps or better accuracy from day to day can be achieved, they can be used to compare the frequency of the L1 clock with the best available frequency standards on the ground. In principle, the average frequency difference over 1 day could be measured to roughly $5 \cdot 10^{-17}$. Since this would be a clock time comparison using two-way measurements, most of the effects of the atmospheric time-delay uncertainty and of spacecraft motion uncertainty would be avoided.

6 Summary

The earliest studies of a dedicated mission aimed mainly at determining the GTD were carried out by the European Space Research Organization during 1969–1973. The mission was called A Space Experiment on Gravitational Theories (SOREL) [21]. A drag-free spacecraft was proposed, and time-delay measurements were to be made when the spacecraft passed behind the Sun. Both microwave tracking and pulsed laser time-delay measurements were assumed. One approach studied was to measure the arrival times of laser pulses against an atomic frequency standard on the spacecraft. The other was to transmit laser pulses back to the ground, and rely less on having a high-accuracy frequency standard onboard.

The type of mission described in the present chapter has much higher accuracy goals than SOREL, and makes use of many technology developments that have occurred in the last three decades or so. One important

difference is the proposal to make use of DRSs similar to those proposed for the LISA mission. Such DRSs are scheduled for flight in 2009 on the LISA Pathfinder mission of the European Space Agency [18,19,22]. However, major improvements in the expected performance at frequencies down to roughly $4 \cdot 10^{-7}$ Hz would be required. Another difference is the proposal to make the measurements from a spacecraft near the L1 point of the Earth–Sun system, to avoid the problem of going through the Earth’s atmosphere.

In the preceding sections, three of the four main error sources for the suggested GTD mission have been discussed. The remaining one, which we have not investigated, is the orbit determination part of the problem. For both spacecraft, the main limitation is likely to be the performance of the disturbance compensation system over periods perhaps twice as long as the 20 days assumed for the main part of the time-delay measurement process. However, the effect of uncertainty in the motion perpendicular to the ecliptic also needs to be considered.

If the round-trip delay can indeed be determined to 0.4 ps in terms of the instantaneous clock frequency, then a measurement of γ from the GTD with an accuracy of 1 or $2 \cdot 10^{-8}$ seems possible. However, the limitations from the disturbance compensation system and the orbit determination problem clearly need to be investigated further.

Acknowledgments

It is a pleasure to thank the following: Stefano Vitale, Bill Weber, Pierre Touboul, Tim Sumner, Diana Shaul, Stephen Merkowitz, and many others for information on the gravitational reference sensors for the LISA and LISA Pathfinder missions; Steve Jefferts, Leo Hollberg, Bill Klipstein, and Christoph Salomon for information on high-stability cesium frequency standards designed for use in space; Jun Ye, Jan Hall, and Judah Levine for discussions of the use of laser pulses, laser comb generators, and laser sideband systems for precise time transfer; Jennifer McGee for assistance with the time-delay calculations; Slava Turyshev and Mike Shao for detailed information on the LATOR mission; Bruno Bertotti, Luciano Iess, and John Armstrong for results concerning the Cassini time-delay measurements; and Irwin Shapiro, Bob Reasenberg, Ken Nordvedt, Jim Williams, Jim Faller, and Bob King for their early enthusiasm concerning testing relativity.

References

1. I.I. Shapiro. *Phys. Rev. Lett.*, 13:789, 1964.
2. J.D. Anderson et al. *Acta Astronautica*, 5:43, 1978.
3. R.D. Reasenberg, I.I. Shapiro, and P.E. MacNeil. *Ap. J.*, 234:L219, 1979.
4. I.I. Shapiro, R.E. Reasenberg, and P.E. MacNeil. *J. Geophys. Res.*, 82:4329, 1977.

5. D.L. Cain, J.D. Anderson, M.S.W. Keeseey, et al. *Bull. Am. Astron. Soc.*, 10:396, 1978.
6. B. Bertotti, L. Iess, and P. Tortora. *Nature*, 425:374, 2003.
7. S.G. Turyshev, M. Shao, and K. Nordtvedt. *Class. Quantum Grav.*, 21:2773, 2004.
8. S.G. Turyshev, M. Shao, and K. Nordtvedt. *Int. J. Mod. Phys.*, D13, 2004.
9. S.G. Turyshev, M. Shao, and K. Nordtvedt. *Proc. XXII Texas Symp. on Relativistic Astrophysics (in press)*. 2005.
10. S. Schiller, A. Goerlitz, A. Nevsky, A. Wicht, C. Lämmerzahl, H.-J. Dittus, S. Theil, P. Touboul, C. Salomon, P. Lemonde, U. Sterr, F. Riehle, E. Peik, G. M. Tino, L. Iorio, I. Ciufolini, E. Samain, A. Peters, W. Ertmer, E. Rasel, L. Maleki, and S. Karshenboim. *Proc. 39th ESLAB Symposium, Noordwijk, 19–21 April 2005, F. Favata, J. Sanz-Forcada, A Giménez eds.*, pages 39–42, 2005.
11. D.B. Sullivan, N. Ashby, E.A. Donley, T.P. Heavner, L. Hollberg, S.R. Jefferts, W.M. Klipstein, W.D. Phillips, and D.J. Seidel. *Adv. Space Res.*, 36:107–113, 2005.
12. Stephen M. Weinberg. *Gravitation and Cosmology*. John Wiley & Sons, New York, 1972.
13. N. Ashby and J. McGee. *to be published*, 2006.
14. K.S. Thorne. *300 Years of Gravitation*. University of Chicago Press, 1987.
15. K. Danzmann and A. Ruediger. *Class. Quantum Grav.*, 20:S1, 2003.
16. *Proc. 5th Int. LISA Symp. & 38th ESLAB Symp.*, (Noordwijk, The Netherlands, 2004); *Class. Quantum Grav.*, 22:S125 through S542, 2005.
17. P.G. Maghami and T.T. Hyde. *Class. Quantum Grav.*, 20:S273, 2003.
18. D. Bortoluzzi et al. *Class. Quantum Grav.*, 20:S89, 2003.
19. S. Anza et al. *Class. Quantum Grav.*, 22:S125, 2005.
20. P.L. Bender. *Class. Quantum Grav.*, 20:S301, 2003.
21. G.M. Israel et al. *SOREL, A Space Experiment on Gravitational Theories: A Report of the Mission Definition Group*, volume MS (73)4. European Space Research Organization, 1973.
22. W. Fichter et al. *Class. Quantum Grav.*, 22:S139, 2005.